

# Raman Spectroscopy in Coatings Research and Analysis: Part I. Basic Principles

by Neil J. Overall, ICI PLC\*

In a previous article in the JCT COATINGS<sup>TECH</sup> Analytical Series, Chalmers discussed the use of infrared (IR) spectroscopy for characterizing and testing coatings.<sup>1</sup> In this two-part companion article, we describe the use of a complementary technique, Raman spectroscopy, for the same purposes. In common with Chalmers, we will not discuss the detailed principles of either small molecule or polymer characterization using Raman (or IR) spectroscopy; there are a large number of excellent review articles and textbooks which fulfill this purpose. Furthermore, we will not cover the basic aspects of Raman spectroscopy for the same reason. Rather, we concentrate on those aspects of Raman spectroscopy that are specific to coating science and technology, expanding on the fundamental principles only when necessary for clarity. Emphasis will be on organic coatings, but some attention will be paid to inorganics too.

With this in mind, Part I of this tutorial attempts to address the following questions:

- What sort of information can be obtained using Raman spectroscopy?
- How is a coating studied in a typical Raman experiment?
- How thin (or thick) of a coating can we study, and what is the influence of the substrate?

After discussing these issues, Part II of this tutorial<sup>†</sup> will focus on mapping or imaging chemical or structural variations in a coating. Examples, drawn both from the literature and the author's own work, will be used to illustrate the capabilities and limitations of the technique.

This tutorial is not intended to be an exhaustive applications review, but hopefully it will indicate the wide variety of chemical and physical characterization problems that can be addressed.

## WHAT INFORMATION CAN BE DERIVED FROM A RAMAN SPECTRUM?

### Interpretation and Identification of Unknowns

The frequency of a Raman (or IR) band is determined by the masses of the atoms in a molecule or crystal, their equilibrium spatial arrangement, their relative displacements during a vibration, and the bond force constants. The

intensity depends on either the change in polarizability (Raman) or dipole moment (IR) during the vibration. Anything that changes the equilibrium shape, the atomic masses, or the force constants (including intermolecular interactions) can change both the frequency and intensity of a band—hence, the sensitivity of vibrational spectroscopy to chemical and physical structure. Different parts of the same molecule tend to be strongly coupled, so changing a single atom in the molecule can perturb many of its vibrations.

This means that a subtle structural change can have a large impact, with the advantage that Raman and IR spectra provide a unique fingerprint for a given molecule in a given conformation. The disadvantage is that it is very difficult to accurately predict the detailed spectrum of any but the simplest molecule. It is simple to use Group Theory to predict the numbers of bands expected in the IR and Raman spectra of molecules<sup>2</sup> or crystals,<sup>3</sup> but it is difficult to predict their absolute frequency or intensity. So, while most undergraduates could give a rather accurate manual prediction of an NMR spectrum of a small molecule, the same task for the vibrational spectrum requires sophisticated computer software. Even then, there will often be significant errors in band positions and intensities. This situation is improving with the widespread availability of user-friendly quantum chemistry software, but even the best available predictions typically have frequency errors of several percent, which equates to several tens of  $\text{cm}^{-1}$ . This is more than enough to cause confusion when trying to rationalize computed and observed spectra.

Most workers who routinely use vibrational spectroscopy do so on the basis of so-called group frequencies. These use the fact that certain groupings tend to give rise to IR or Raman bands that fall within well defined ranges, irrespective of the structure of the rest of the molecule. Numerous tabulations of group frequencies are available that can help identify the likely functional groupings that are present in an unknown material,<sup>4-6</sup> but because many of the bands are due to collective vibrations throughout a molecule, it is usu-

\*Measurement Science Group, The Wilton Centre, Wilton, Redcar, TS104RF, UK.

†To be published in the September 2005 issue of JCT COATINGS<sup>TECH</sup>.

ally impossible to assign the origin of every band in a spectrum (nor is it necessary for general purposes).

In practice, for many workers the first course of action when confronted by an unknown spectrum is to use spectral searching software to match the unknown to a database of reference spectra. Undoubtedly, this is a very useful approach, but it is worth getting into the habit of checking the spectra of any potential matches using the functional group approach, just to ensure that the results make sense. Most seasoned vibrational spectroscopists have their own favorite examples of misleading results thrown up by databases, often due to mislabelling of reference spectra. In these cases, even a cursory functional group analysis could avoid an embarrassing mistake. A more serious problem is the comparative paucity of electronic Raman reference data; this is improving with time as Raman becomes a more common analytical technique.

### Composition and Structure

Often a worker has a good idea of the general classification of a material, but requires information on more subtle issues of composition. These could include nature and relative amount of comonomers, molecular conformation and configuration, presence of additives and fillers, end groups, sequence and branching, degree of cure/degree of polymerization, residual monomer, and blend composition. Raman spectroscopy offers information on all of these properties, to a greater or lesser extent. One can also probe physical properties, including molecular orientation, degree of crystallinity, polymorphs or allotropes, crystal and domain size, crystal defects, and stress/strain. Coat thickness and uniformity can also be measured in favorable circumstances.

### Quantitation

The band intensity depends on the concentration of scattering species in the laser beam, so Raman spectroscopy is, in principle, a quantitative technique. There is often a linear relationship between concentration and band intensity, but the constant of proportionality must be obtained by calibration using materials of known composition. It is unwise simply to assume that if the band intensity doubles or halves,

then the concentration varies to the same extent; one needs to prove a linear relationship before making this assertion. Furthermore, many factors can affect the absolute band intensity; for example, laser power, alignment of the sample and collection optics, and the throughput of the spectrometer. Unlike Fourier transform infrared (FTIR) spectroscopy, where the sample spectrum is normalized using a background curve to yield an absolute transmission or absorbance spectrum, Raman is a single beam technique; there is no equivalent normalization process. This means that measuring the same sample from day to day could give very different intensities. To compensate, in practice one normally uses a reference band to normalize the spectral intensity. The normalization band could be from a solvent, or from another component in a mixture. The ratio of the analyte band to the reference band should then only vary with the analyte/reference concentration ratio.

Figure 1 illustrates this approach using the example of a terpolymer of styrene (S), methyl methacrylate (MMA), and butyl acrylate (BuA).<sup>7</sup> A set of samples that were prepared with different monomer ratios were first analyzed using NMR spectroscopy to accurately determine the composition. The Raman spectra were then calibrated in a two-step process. First, the intensity ratio of the 842 and 812  $\text{cm}^{-1}$  Raman bands (which arise from C-C vibrations from the respective polymerized monomers) was correlated with the BuA/MMA mass ratio. This gives a calibration for the ratio of the two acrylic monomers. Then, the styrene/total acrylic mass ratio  $[S/(BuA+MMA)]$  was correlated with the intensity ratio of the 1603  $\text{cm}^{-1}$  (pendant aromatic) and 1731  $\text{cm}^{-1}$  (ester carbonyl) bands. Figure 1 shows the quality of fit for both calibrations. In fact, the  $S/(BuA+MMA)$  fit is somewhat

fortuitous, since it relies on the fact that the ester carbonyl intensity happens, in this case, to depend solely on the combined mass of BuA and MMA present (i.e., it is insensitive to the monomer type). If this were not the case, we could instead ratio the 1603  $\text{cm}^{-1}$  styrene band against the 812  $\text{cm}^{-1}$  (MMA) or 842  $\text{cm}^{-1}$  (BuA) bands to give two separate correlations.

This calibration was necessary because, in practice, these materials are crosslinked using a functionalized acrylate as a fourth monomer. The crosslinked product is insoluble and intractable to NMR analysis, but the crosslinker is at too low a level to invalidate the NMR-Raman calibration. Therefore, we can use the calibrated Raman technique to analyze commercial materials (including the degree of crosslinking, by monitoring consumption of the pendant crosslinker). This is a useful general approach—use a high information content, primary technique such as NMR to provide detailed quantitative structural information, calibrate Raman spectra using the NMR data, and then apply Raman spectroscopy in situations where the primary technique is inapplicable. The primary technique could be compositional (often NMR or a set of manually prepared mixtures), or

Figure 1—Calibration of Raman data for the composition of a styrene-butylacrylate-methylmethacrylate terpolymer. Calibration is a two-step process: first the styrene/total ester ratio, then the MMA/BuA ratio. Fortuitously in this case, the ester carbonyl intensity only depends on the total mass fraction of ester present, not on the ester speciation. Redrawn from Figure 4.10 of reference 7, with permission from Blackwell Press.

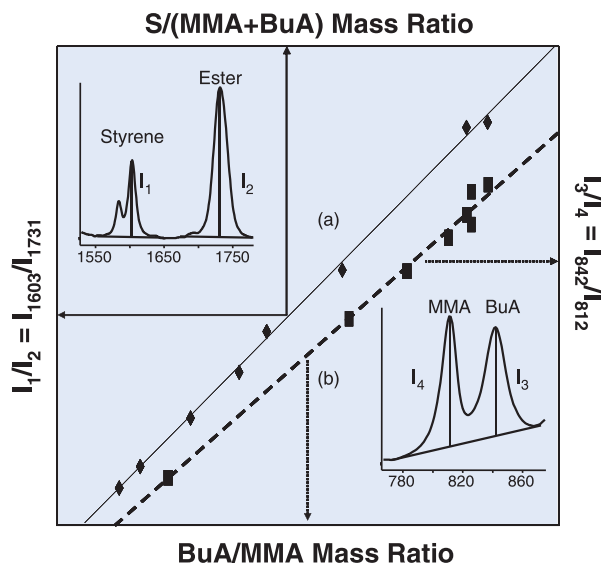
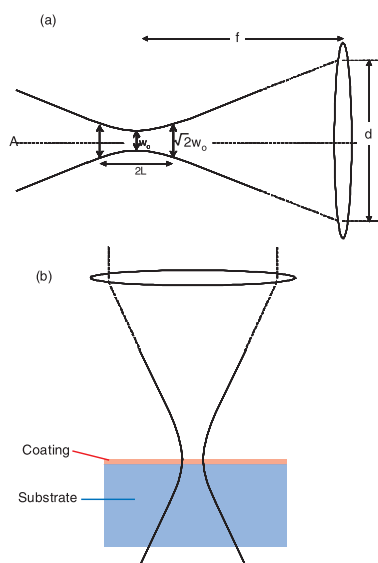


Figure 2—(a) Shape of the focal volume of a Gaussian laser beam in air and (b) under-filling of beam focus by a thin coating on a thick substrate. Both diagrams not to scale.



physical (X-ray diffraction, density, thermal analysis, etc).

Selection of an acceptable reference band is very important. In a simple mixture of non-interacting components, almost any non-overlapped band from a known component is acceptable. The band ratio should vary linearly with the component ratios, as shown in Figure 1. Difficulties arise when components interact differently at different concentrations. With copolymers, we sometimes find that, as the concentration ratio varies, we move from a random to a blocky sequence, so the intrinsic band intensities change as a result. This would be manifested as a nonlinear calibration curve. For another example, it might be tempting to use one of the water Raman bands as a reference for aqueous solutions, but the intrinsic intensity and shape of the water bands usually depends on the solute concentration. This is because the water structure is perturbed by the dissolved species.

A rather different problem arises when trying to monitor the extent of a chemical reaction. One measures loss of a reactive species (such as C=C), but needs a reference band from a vibration that is not strongly coupled to the reactive group. Otherwise, the intrinsic intensity of the reference band will change during the reaction. The polymerization of styrene is a good specific

example; one can easily follow the loss of the vinyl C=C group ( $\sim 1630\text{ cm}^{-1}$ ), but this group is conjugated to the aromatic ring, so the nearby  $1602\text{ cm}^{-1}$  ring band changes intensity very dramatically when the C=C bond reacts. In fact, the  $1602\text{ cm}^{-1}$  band is over five times more intense in the monomer than it is at the same concentration in the polymer, due to the loss of conjugation on reaction, so it makes a wholly unsuitable internal standard.<sup>8</sup> In this case, a solvent band would provide a more reliable reference. The quantitative effect on a calibration curve of a non-constant reference band has been discussed in detail elsewhere.<sup>7</sup>

Finally, we should mention that there are a variety of calibration techniques that do not require manual selection of Raman bands for the analytes of interest. Among the most popular are the multivariate methods such as partial least squares analysis (PLS). These methods automatically select bands that correlate well with the property of interest, which could be compositional, as above, or a physical property such as crystallinity. However, even these methods require a normalization step, to account for the large variations in overall spectral intensity that can occur when measuring the same sample from day to day. One method that we have found to work well is to normalize the total area under each spectrum (or the spectral range of interest) to unity. We have used this approach to build PLS models to measure the crystallinity of poly(ethylene terephthalate) (PET) and poly(ethylene) (PE) from their Raman spectra.<sup>9,10</sup> Alternatively, the user can select an appropriate reference band to scale the spectra. Vickers and Mann have given a useful summary of factors to be considered for quantitative Raman spectroscopy.<sup>11</sup>

### Ordering in Semi-Crystalline Systems

When a polymer crystallizes, significant lengths of the chain adopt a regular, extended conformation, and these ordered lengths become aligned to form a regular lattice in three dimensions. Crystallization therefore involves intramolecular and intermolecular ordering. The change in conformation has by far the largest effect on the vibrational spectrum; this is because the shape of the molecule is a major factor in determining the band frequency and intensity. The 3D alignment of neighboring

chains usually has a much smaller effect due to the relative weakness of intermolecular interactions, although strong interactions (such as intermolecular H-bonding in polyamides) can have a large effect on band positions and intensities. Weak interactions are often manifested by band splitting as the local symmetry becomes reduced; a classic case is the splitting of the IR band at  $720\text{ cm}^{-1}$  in the spectrum of poly(ethylene). In fact, many of the spectral changes that have been attributed to polymer crystallization should be more correctly referred to as regularity bands, arising from conformation rather than chain packing. One rarely obtains a direct measure of crystallinity from a vibrational spectrum, and this can cause confusion in cases where one can vary the conformation without inducing crystallization. For example, PET can be cold-drawn to produce highly extended, regular polymer chains but without generating the intermolecular registration required for crystallization.<sup>12</sup> The distinction between conformation, regularity, and crystallinity effects was clearly made long ago,<sup>13</sup> but incorrect terminology and confusion still occur occasionally in the literature.

## SAMPLING CONSIDERATIONS

### General

The infrared spectroscopist has a diverse array of sampling techniques for surface analysis.<sup>1</sup> For example, it is trivial to selectively examine the surface  $1\text{ }\mu\text{m}$  of a material using Attenuated Total Reflection (ATR)-FTIR spectroscopy. In contrast, it is actually rather difficult to obtain a pure Raman spectrum on the same scale, so in that sense Raman spectroscopy is less suited for routine surface analysis. Most Raman experiments use a lens to focus a laser beam onto a sample (exceptions being near-field Raman spectroscopy,<sup>14</sup> some fiber optic probe designs,<sup>15</sup> and total internal reflection spectroscopy<sup>16</sup>). A focused laser beam has a diffraction-limited waist given by  $w_0 = 2f\lambda/d$ , where  $f$  is the focal length of the lens,  $\lambda$  is the laser wavelength, and  $d$  is the diameter of the collimated laser beam (Figure 2a). Note,  $w_0$  can be submicron when a high power microscope objective is employed. The beam remains approximately collimated (within a factor of  $\sim 1.4$ ) to a distance  $L$  on either side of the focal plane ( $L = \pi w_0^2/2\lambda$ ). This simple picture neg-



lects the influence of the discontinuity in refractive index when a sample is placed in the beam (more will be discussed on this later). If the laser beam fills the focusing lens (the usual case when a microscope objective is used), the size of this focal volume roughly determines the best attainable spatial resolution (and, hence, the thinnest coating that can be analyzed without substantial contributions from surrounding material). Ideally, we would like to arrange for the sample to at least fill the laser focal volume.

Most modern Raman systems use a back-scattering geometry, so the lens which focuses the laser beam also collects the Raman light and projects an image back onto the entrance slit of the spectrometer. In any Raman experiment, there is a significant intensity of Raman scatter generated outside of the nominal laser focal volume, and this light can also be relayed back through the entrance slit to the detector (albeit with lower efficiency).

### Practical Arrangements for Analyzing Coatings

Figure 2b illustrates the simplest method of studying a coating, namely focusing the laser directly onto the surface. Matching the laser focal volume to the coat thickness is important. Unless it is very thick, a coating will usually be studied using a microscope objective. In our laboratory, we typically use a 10x microscope objective for "macroscopic" sampling, or a 50x or 100x objective for microscopic analysis. A 1 cm focal length objective, focusing a 2 mm diameter, 500 nm laser beam is calculated to give a beam focus with a waist  $w_0 \sim 5 \mu\text{m}$  and length  $2L \sim 0.2 \text{ mm}$ . Longer focal length objectives quickly lose depth resolution. It is possible to study coatings that are much thinner than the depth of focus of the objective, but the data will suffer from poor signal to noise, and excessive contributions from the substrate. Nonetheless, if the substrate is highly reflective, or a weak or inactive Raman scatterer, or if the coating is an exceptionally strong Raman scatterer, then it may be possible to obtain a reasonable spectrum of a thin coating that does not fill the laser focus.

In summary, selecting the correct focusing optic is a compromise between correctly filling the laser focal volume so as to obtain the desired spatial resolution, and the desire to work with the

highest  $f\#$  objective possible to maximize collection efficiency. The  $f\#$  is simply the lens focal length divided by its diameter. A high power microscope objective would typically have  $f/0.15$  (that is,  $f\#=0.15$ ), while a sampling lens used for laboratory macroscopic measurements might lie between  $\sim f/0.9$  and  $\sim f/2$ . Pelletier has summarized the relationship between  $f\#$ , collection efficiency, and the considerations involved in selecting optics that maximize throughput through the spectrometer,<sup>17</sup> while another excellent text is available which discusses in fine detail the optical design and performance of Raman spectrometers and microscopes.<sup>18</sup>

### Depth Profiling Coatings: Confocal versus Mechanical Sectioning

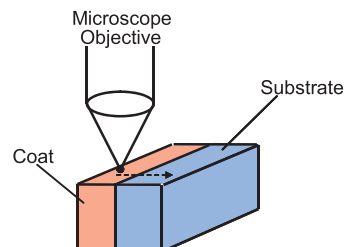
To measure the average composition of a coating, ideally one would match the collimation length  $2L$  to the coat thickness. Thus, a low power lens coupled to a spectrometer which does not have a microscope might be perfectly adequate. If a much tighter laser focus is used, one would need to sample at many different positions in order to estimate the average composition.

However, if the spatial variations are of interest, a higher power objective, coupled to a Raman microscope, will be needed to map or image the sample.<sup>19,20</sup> This can be very time-consuming, depending on the spatial resolution required and the area of sample to be studied, but the ability to probe the microstructural details of a coating is one of the key advantages of Raman microscopy. It is worth considering this point in some detail.

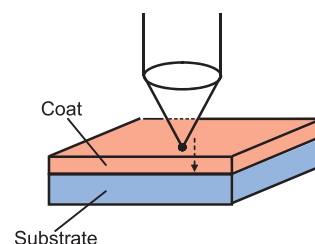
Let us imagine that one is interested in depth profiling the composition of a coating with the best possible spatial resolution. There are two ways this could be attempted with a Raman microscope. First, one could section or polish a smooth cross-section of the sample, and map across the sample, collecting data point by point (Figure 3a). In this case, which is sometimes referred to as lateral profiling, the spatial resolution is determined mainly by the waist diameter  $w_0$ , although there will be contributions from light above and below the plane of tightest focus, which will cause some blurring. The second approach, which in principle is very attractive since it requires no sample preparation, is simply to focus directly

Figure 3—Options for depth profiling a heterogeneous material: (a) lateral scanning of a mechanically prepared (i.e., microtomed, fractured, or polished) cross-section, and (b) optical (axial) sectioning using a confocal microscope. The benefits and disadvantages of each approach are discussed in detail in the text.

(a) Mechanical Cross-section (Lateral Scan)



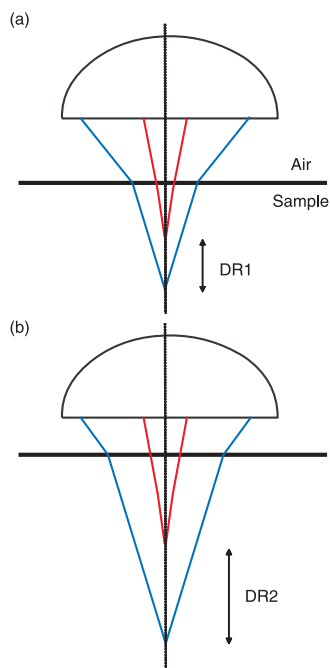
(b) Optical Section (Axial Scan)



onto the surface of the sample and move the focus incrementally downwards towards the substrate, collecting spectra along the way (Figure 3b). (Obviously, this approach is restricted to transparent samples.) The idea behind this axial profiling is that the calculated laser focal volume is of the order of  $1 \mu\text{m}^3$  for a high power objective, so we have a tiny probe that can be moved around to measure subsurface structure with very high spatial resolution, without requiring any sample preparation. Use of a confocal aperture at a back focal plane of the microscope will further sharpen the focus, restricting detection of light originating away from the focal plane.<sup>21</sup>

The problem with this approach is that for most Raman microscopes, Figure 2a is not a valid description once a sample is placed in the laser beam. The problem is outlined schematically in Figure 4. When the laser rays enter the sample they suffer refraction, and the marginal rays are focused deeper than the paraxial rays, an effect known as spherical aberration.<sup>22-24</sup> The net result is that the laser focus becomes blurred along the axis normal to the sample surface, and the position of focus shifts significantly deeper within the

Figure 4—Effect of spherical aberration when using with a high power metallurgical objective to focus a laser beam beneath the surface of a transparent sample. Marginal rays are focused more deeply than paraxial rays, and the discrepancy, or depth resolution (DR), worsens the deeper one attempts to focus. DR can be tens of microns.



sample. The focal blurring becomes worse the deeper one attempts to focus ( $DR2 > DR1$ ), and the confocal aperture is only partially effective in maintaining the depth resolution of the instrument.<sup>24</sup> The problem is most pronounced with high power objectives (just the situation with a typical Raman microscope). The problem arises because almost all commercial Raman microscopes are sold with metallurgical objectives designed to focus onto the surface of an opaque sample. They are not corrected for the aberrations that occur when focusing into a transparent sample. The problem can be minimized either by using an objective that is designed to function when focusing through an overlayer of transparent material, such as an oil immersion objective,<sup>23,25</sup> or by using a dry objective that is corrected for a cover slip,<sup>26</sup> and many more researchers are now aware of the problem and are taking steps to minimize it. However, the worker who is new to the field should be aware that there are many papers in the literature that ignore this effect, and contain depth profiles where the depth axis might be incorrect by a factor of two or

more, and where the claimed depth resolution is grossly overestimated. Furthermore, one can still find modern papers that claim that a confocal Raman microscope is capable of selectively analyzing  $1 \mu\text{m}^3$  of material inside a transparent sample, and this is generally incorrect.

A recent two-part article has summarized the key issues that arise with axial confocal Raman depth profiling with a metallurgical objective.<sup>27,28</sup> The main points are:

- With a typical high power microscope objective, the laser focus lies deeper than you think; typically by a factor of  $\sim 2$ .
- Spherical aberration spreads the laser field over a considerable distance along the axis; the depth resolution is degraded, and gets worse as one focuses deeper.
- Depending on the position of a buried feature, its apparent thickness (according to the raw intensity-depth profile) can be underestimated, overestimated, or about right, depending on the interplay between the position of the laser focus and the changing depth resolution.
- The effects can be modeled using models of varying degree of complexity, but this is time-consuming and demands quite a lot of knowledge of the sample structure beforehand, especially the refractive index of different layers. Modeling data from a completely unknown sample would be difficult.
- Using a corrected objective (e.g., oil immersion) can significantly reduce the problems and yield more easily interpretable depth profiles.

In my experience, axial profiling with a metallurgical objective is more likely to result in a depth resolution of  $5\text{--}10 \mu\text{m}$  or worse, rather than the  $1 \mu\text{m}$  often claimed in the literature. Furthermore, it is arguable that if one has the choice, mechanical sectioning and lateral scanning is preferable, since one knows exactly where one is focused without the need for complex modeling or special objectives. Even if one could eliminate all of the aberrations associated with axial profiling, lateral scanning will always have a better

spatial resolution simply because the laser waist  $w_0$  is always smaller than the focal length ( $\pi w_0^2/\lambda$ ). The exception to this rule would be where mechanical sectioning will disturb the structure of interest.

Figures 5 and 6 illustrate these points. Figure 5 shows how the apparent thickness of a thin layer is much greater when it is on the bottom of a sample rather than the top, due to the greater blurring of the laser focus with increasing depth. A laminate consisting of a  $\sim 10 \mu\text{m}$  layer of PEN [poly(ethylenephthoate)] on a  $180 \mu\text{m}$  PET film was used to demonstrate the effect. When the laser was focused directly onto the PEN, its apparent thickness was  $\sim 5 \mu\text{m}$ , but this increased to  $\sim 18 \mu\text{m}$  when the laser was focused through the PET substrate onto the PEN. Therefore, the perceived thickness of an object clearly depends on its depth below the sample surface.

Figure 6 shows another experiment designed to test which configuration has the best spatial resolution, by measuring the apparent thickness of a sharp interface between two polymers. Raman data was taken through the interface between a  $20 \mu\text{m}$  layer of PE on a  $100 \mu\text{m}$  PET substrate. Clearly the spatial resolution, as judged from the rate of change of the PE signal on moving through the boundary, was better (by a factor of two) using lateral scanning of a cross-sectioned sample. The resolution of configuration (b) will be further worsened the thicker the top layer is, as demonstrated in Figure 5.

Figure 5—A simple demonstration of the degradation of confocal Raman depth resolution with increasing sampling depth. The same layer appears to be much thicker when one focuses through a thick polymer substrate (ii) rather than directly on the coating layer (i).

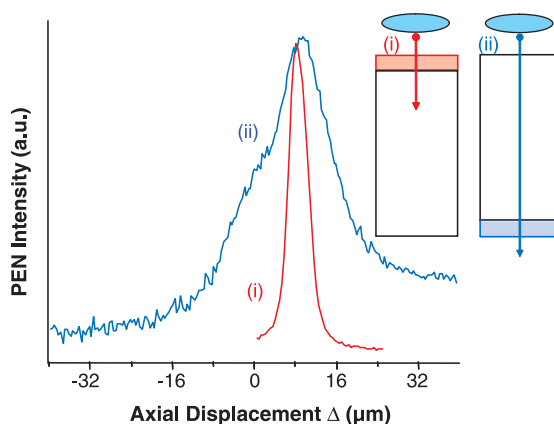


Figure 6—A comparison of the resolution of lateral and axial configurations by scanning through a PE-PET interface. The PE layer was  $\sim 20\ \mu\text{m}$  thick. The lateral scanning resolution (a) was twice as good as that of axial scanning (b). The axial resolution will worsen as the over-layer thickness increases (see Figure 5).

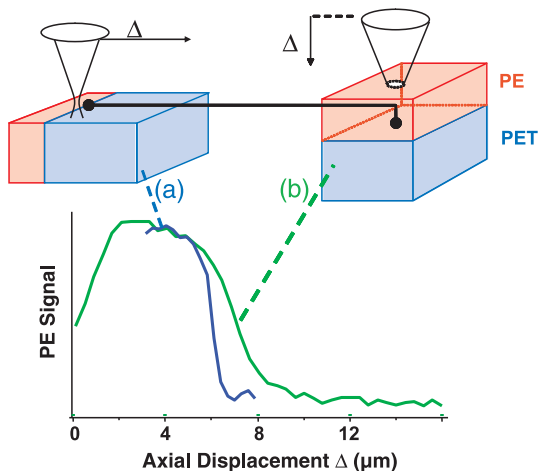
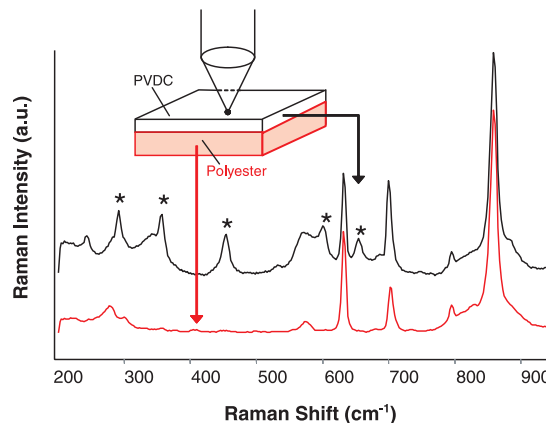


Figure 7—The surface specificity of confocal Raman microscopy illustrated by a spectrum of a  $2\ \mu\text{m}$  layer of PVDC on a polyester substrate, compared with a spectrum of the pure polyester. Strong features due to the substrate are clearly present in the coating spectrum, which shows that the surface specificity is somewhat worse than  $2\ \mu\text{m}$ . The PVDC bands are marked with asterisks.



Despite these problems, the experimental simplicity of the confocal approach remains a significant attraction. If one chooses to use this method, then ideally one should minimize the aberrations—for example, by using an immersion objective. This can also enable the acquisition of data from subsurface regions of opaque samples, provided the material is porous. This is because immersion oil can penetrate into the pores, and wet-out the discontinuities in refractive index which cause turbidity. Vyorykka et al. showed how an immersion objective permitted data acquisition from deep within papers and polymers with opaque coatings.<sup>29</sup> If spherical aberration cannot be avoided, then a numerical correction should be applied to the depth scale to account for the shift of the laser focus deeper into the sample. The effect of the change in the depth resolution can be minimized by normalizing the Raman band intensities using a reference band that is approximately invariant. For example, if one were monitoring diffusion of a surface-treatment into a polymer, the apparent intensity of the dopant band could be normalized using a polymer band. The use of normalization has been discussed by other workers<sup>30</sup> and offers some promise, although it obviously requires presence of a band that is invariant throughout the coat thickness, and this simply is not available in some cases (e.g., a laminate with chemically distinct layers).

It is worth pointing out that, even in the absence of spherical aberration, the notion that confocal Raman microscopy has a depth resolution of  $\sim 1\ \mu\text{m}$  is incorrect. This is because some light from either side of the laser focal volume will be transmitted to the detector, particularly the light that runs very close to the optical axis of the system (line labeled "A" in Figure 2). This means that when focusing directly onto the surface of a sample, spectral features can be detected from several microns below the surface, and this is true even for confocal Raman microscopy. To illustrate this point, Figure 7 shows the spectrum of a  $2\ \mu\text{m}$  coating of PVDC [poly(vinylidene chloride)] on a polyester substrate, compared with a spectrum of the polyester alone. The PVDC bands are marked with an asterisk. Conventional wisdom implies that a pure spectrum of PVDC should be expected, but this is not found; the polyester bands are substantial. In fact, if one has a coating that is a weak Raman scatterer on a strongly Raman active substrate, one can find that the substrate signal can dominate even when the coating is thick ( $10\ \mu\text{m}$  or more). In short, it can be very difficult to obtain a pure Raman spectrum of a coating using the confocal configuration.

The data shown in Figure 7 clearly illustrate the fact that, in general, Raman spectroscopy is far less surface-specific than IR spectroscopy. It is trivial to ob-

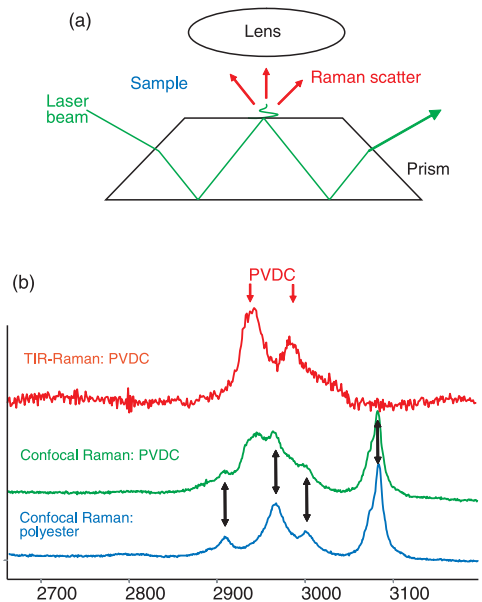
tain a pure FTIR spectrum of the surface  $1\ \mu\text{m}$  of a material using an inexpensive FTIR spectrometer and an internal reflection accessory,<sup>1</sup> but a confocal Raman microscope that is an order of magnitude more expensive cannot approach this degree of surface specificity.

### Improving Surface Specificity: Total Internal Reflection (TIR) Raman Spectroscopy

With infrared internal reflection spectroscopy, a beam of light suffers total internal reflection at the base of a high refractive index, infrared-transparent optical prism.<sup>1</sup> In this configuration, an evanescent wave extends a short distance beyond the prism and can penetrate into a sample placed on its surface. Similarly, if a laser beam, rather than infrared light, is made to suffer total internal reflection, it is possible to generate Raman scatter from the surface of a sample in contact with the prism (Figure 8a). Raman scattering from evanescent waves was first demonstrated by Ikeshoji et al.<sup>31</sup> In principle, internal reflection Raman spectroscopy should have even greater surface specificity than internal-reflection infrared spectroscopy, because the penetration depth of the evanescent light is proportional to its wavelength. Submicron specificity should therefore be readily attainable for TIR-Raman spectroscopy. Greene and Bain have shown how TIR-Raman



Figure 8—(a) Schematic showing optical configuration for TIR-Raman spectroscopy. In the configuration shown, the Raman scatter is collected from the prism/sample interface by focusing the collection objective through the (transparent) sample. Opaque samples can be studied by focusing the objective through the opposite prism face. (b) Comparison of a TIR-Raman spectrum of PVDC-coated polyester, a confocal Raman spectrum of PVDC-coated polyester, and a confocal Raman spectrum of the polyester—all in the C-H stretching region. The TIR-Raman configuration generates a pure spectrum of the PVDC, whereas the confocal Raman spectrum is heavily contaminated with bands from the substrate (marked with arrows).



spectroscopy can analyze polymer surfaces with better surface specificity than confocal Raman microscopy, using the example of a 5 micrometers layer of PEN coated onto PET.<sup>16</sup> The TIR-Raman approach was able to fully resolve the upper PEN layer, while the confocal Raman spectrum of the PEN layer was still contaminated by PET features.

A more rigorous test of the surface specificity is exemplified in Figure 8b, which compares the TIR-Raman and confocal Raman spectra from the PVDC/polyester laminate layer in the C-H stretch region. (The data are restricted to this region, rather than the 200–900  $\text{cm}^{-1}$  range shown in Figure 7, because the zirconia prism used as the internal reflection element had a broad Raman background between 300–800  $\text{cm}^{-1}$ , which masks the PVDC features). In contrast to the confocal spectrum, which is dominated by the polyester bands, the TIR-Raman spectrum contains only PVDC bands. This proves that

the penetration depth was significantly less than 2  $\mu\text{m}$ , and, hence, superior to confocal Raman microscopy.<sup>32</sup> Unfortunately, the signal/noise of the TIR Raman spectrum was quite poor, owing to the use of a 532 nm laser, which generated significant sample fluorescence. This could be overcome by using a high power red or near-infrared laser for excitation.

It remains to be seen whether TIR Raman will gain popularity as a routine analytical tool. There are some significant barriers to uptake, such as the need for a high power laser (compared with current conventional instruments), the lack of convenient optical materials with high refractive index but low Raman and fluorescence cross-sections, and the lack of a commercially available instrument or accessory. It does, however, offer the only Raman configuration with submicron surface specificity that does not rely on a special effect such as surface enhanced scattering or resonance Raman enhancement to provide the resolution.

Applications using both of these phenomena will be discussed in Part II of this tutorial. [□](#)

## References

- (1) Chalmers, J.M., "Infrared Spectroscopy in the Analysis, Characterization, and Testing of Coatings," *JCT CoatingsTech*, 2, No. 18, 50 (2005).
- (2) Cotton, F.A., *Chemical Applications of Group Theory*, John Wiley and Sons, New York, 1990.
- (3) Fateley, W.G., Dollish, F.R., McDevitt, N.T., and Bentley, F.F., *IR and Raman Selection Rules for Molecular and Lattice Vibrations*, Wiley Interscience, New York, 1972.
- (4) Mayo, D.W., Miller, F.A., and Hannah, R.W., *Course Notes on the Interpretation of IR and Raman Spectra*, Wiley Interscience, New York, 2004.
- (5) Lin-Vien, D., Colthup, N.B., Fateley, W.G., and Grasselli, J.G., *Handbook of IR and Raman Characteristic Group Frequencies*, Academic Press, New York, 1991.
- (6) Socrates, G., *IR and Raman Characteristic Group Frequencies, 3rd Ed.*, John Wiley and Sons, Chichester, 2001.
- (7) Everall, N.J., in *Analytical Applications of Raman Spectroscopy*, Pelletier, M.J. (Ed.), Blackwell Science, Oxford, pp. 127-192, 1999.
- (8) Wang, C., Vickers, T.J., Schlenoff, J.B., and Mann, C.K., *Appl. Spectrosc.* 46, 1729 (1992).
- (9) Everall, N., Taylor, P., Chalmers, P., Mackerron, D., Ferwerda, R., and van der Maas, J.H., *Polymer*, 35, 3184 (1994).
- (10) Williams, K.J.P. and Everall, N.J., *J. Raman. Spectrosc.*, 26, 427 (1995).
- (11) Vickers, T.J. and Mann, C.K., in *Analytical Raman Spectroscopy*, Grasselli, J.G. and Bulkin, B.J. (Eds.), John Wiley and Sons, New York, 1991.
- (12) Adar, F. and Noether, H., *Polymer*, 26, 1935 (1985).
- (13) Zerbi, G., Ciampelli, E., and Zamboni, V., *J. Polym. Sci. C.*, 141 (1964).
- (14) Kawata, S. and Inouye, Y., in *Handbook of Vibrational Spectroscopy*, Vol. 2, Chalmers, J.M. and Griffiths, P.R. (Eds.), John Wiley and Sons, Chichester, pp. 1460-1471, 2002.
- (15) Lewis, I.R. and Lewis, M.R., in *Handbook of Vibrational Spectroscopy*, Vol. 2, Chalmers, J.M. and Griffiths, P.R. (Eds.), John Wiley and Sons, Chichester, pp. 1587-1597, 2002.
- (16) Greene, P.R. and Bain, C.D., *Spectroscopy Europe*, 16, 8 (2004).
- (17) Pelletier, M.J., in *Analytical Applications of Raman Spectroscopy*, Pelletier, M.J. (Ed.), Blackwell Science, Oxford, pp. 53-105, 1999.
- (18) *Raman Microscopy: Developments and Applications*, Turrell, G. and Corset, J. (Eds.), Academic Press, New York, 1996.
- (19) Dhamelincourt, P., in *Handbook of Vibrational Spectroscopy*, Vol. 2, Chalmers, J.M. and Griffiths, P.R. (Eds.), John Wiley and Sons, Chichester, pp. 1419-1428, 2002.
- (20) Treado, P.J. and Nelson, P., in *Handbook of Vibrational Spectroscopy*, Vol. 2, Chalmers, J.M. and Griffiths, P.R. (Eds.), John Wiley and Sons, Chichester, pp. 1429-1459, 2002.
- (21) Tabaksblat, R., Meier, R., and Kip, B.J., *Appl. Spectrosc.*, 46, 60 (1992).
- (22) Everall, N.J., *Appl. Spectrosc.*, 54, 1515 (2000).
- (23) Everall, N.J., *Appl. Spectrosc.*, 54, 773 (2000).
- (24) Baldwin, J.K. and Batchelder, D.N., *Appl. Spectrosc.*, 55, 517 (2001).
- (25) Froud, C.A., Hayward, I.P., and Laven, J., *Appl. Spectrosc.*, 57, 1468 (2003).
- (26) Adar, F., Naudin, C., Whitley, A., and Bodnar, R., *Appl. Spectrosc.*, 58, 1136 (2004).
- (27) Everall, N.J., *Spectroscopy* 19, 22 (2004).
- (28) Everall, N.J., *Spectroscopy* 19, 16 (2004).
- (29) Vyorykka, J., Halttunen, M., Litti, H., Tenhunen, J., Vuorinen, T., and Stenius, P., *Appl. Spectrosc.*, 56, 1123 (2002).
- (30) Reinecke, H., Spells, S.J., Sacristan, J., Yarwood, J., and Mijangos, C., *Appl. Spectrosc.*, 55, 1660 (2001).
- (31) Ikeshoji, T., Ono, Y., and Mizuno, T., *Appl. Opt.*, 12, 2236 (1973).
- (32) Bain, C.D., MacMillan, C., and Everall, N., unpublished data, 2004.